Measurements of fluctuation-induced diamagnetism above the superconducting transition in $YBa_2Cu_3O_{7-\delta}$ single crystals in low magnetic fields: Comparison with paraconductivity

C. Torrón, A. Díaz, A. Pomar, J. A. Veira, and Félix Vidal

Laboratorio de Física de Materiales, Departamento de Física de la Materia Condensada, Facultad de Física, Universidad de Santiago, Santiago de Compostela, 15706 Spain

(Received 19 April 1993; revised manuscript received 30 November 1993)

We report detailed experimental results on the magnetic susceptibility of high-quality $YBa_2Cu_3O_{7-\delta}$ single crystals for the applied magnetic field H parallel, χ_{ab}, and perpendicular, χ_c, to the c direction. The data were obtained from 5 to 300 K, and with $\mu_0 H \leq 0.6$ T, for which χ_{ab} and χ_c above the superconducting transition correspond to the so-called weak magnetic-field limit, even for reduced temperatures, $\varepsilon \equiv (T - T_{CO})/T_{CO}$, of the order of $\varepsilon = 2 \times 10^{-3}$, where T_{CO} is the mean-field-like normal-superconducting transition temperature. For $T > T_{CO}$, χ_c is found to be temperature independent and its average value for the samples measured here is $(2.7 \pm 0.5) \times 10^{-5}$. In contrast, $\chi_{ab}(T)$ is found to be temperature independent, and equal to $(5.2 \pm 1) \times 10^{-5}$, only above $T - T_{CO} \approx 25$ K and up to the highest temperature studied here (300 K). Between T_{CO} and $T - T_{CO} \approx 25$ K, $\chi_{ab}(T)$ is appreciably rounded. The excess diamagnetism above but near T_{CO}, for H parallel to the c axis, $\Delta\chi_{ab}$, is analyzed in terms of the existing approaches for independent Gaussian fluctuations of the superconducting-order-parameter amplitude in layered materials and also compared with the paraconductivity measured in the same samples. The so-called mean-field-like region will correspond to, approximately, $10^{-2} \lesssim \varepsilon \lesssim 0.15$. Beyond the lower ε limit, closer to T_{CO}, both the paraconductivity and $\Delta\chi_{ab}(\varepsilon)$ separate from the mean-field region behavior. Although so close to the transition we cannot exclude the influence of small stoichiometric inhomogeneities, these data for $\varepsilon \lesssim 10^{-2}$ may be explained on the grounds of the three-dimensional XY model, with a critical exponent of $x = -\frac{1}{3}$ for the paraconductivity and $x = -\frac{2}{3}$ for the fluctuation-induced diamagnetism. A scenario compatible with the experimental results is characterized by the values of the correlation length amplitude in the ab plane and in the c direction of, respectively, $\xi_{ab}(0) = (1.1 \pm 0.2)$ nm and $\xi_c(0) = (0.12 \pm 0.02)$ nm, two Josephson coupled superconducting planes in the unit-cell length, and a complex order parameter with two real components, i.e., conventional $^1s_0$-wave pairing or one-complex-component unconventional pairing.

I. INTRODUCTION

High-precision data on the influence of the superconducting-order-parameter fluctuations (OPF) on the magnetic susceptibility $\chi(T)$ in the zero magnetic-field limit, will help in the understanding of the superconducting transition in copper-oxide materials.[1-3] In particular, when combined with data on the paraconductivity in the mean-field-like region (MFR) above the superconducting transition, the fluctuation-induced diamagnetism $\Delta\chi$ in that MFR may serve to check some general aspects of the superconducting pairing state and to obtain useful relationships between some of the characteristic lengths arising in the Ginzburg-Landau-like descriptions of the superconducting transition.[4] At present there exist various high-precision data of the electrical resistivity in the ab plane $\rho_{ab}(T)$ obtained in good $YBa_2Cu_3O_{7-\delta}$ single crystals,[5-12] from which it is possible to extract the paraconductivity in the ab plane $\Delta\sigma_{ab}(T)$. In addition, recently we have obtained the paraconductivity in the a direction (not affected by the presence of the CuO chains) $\Delta\sigma_a(T)$ from resistivity measurements in $YBa_2Cu_3O_{7-\delta}$ single crystals having a large untwinned region in their centers. This makes possible the use of an electrical arrangement with the untwinned part between the voltage contacts (see below).[13] In contrast, most of the available $\chi(T)$ data in the $YBa_2Cu_3O_{7-\delta}$ compound have been obtained in polycrystal films, in granular samples[4,14-16] and in single crystals probably affected by appreciable inhomogeneities,[17-19] or by using high magnetic fields, which complicate the OPF analysis.[20-22]

The main aim of this paper is to present high-resolution measurements, in the so-called weak magnetic-field limit,[3] of the magnetic susceptibility for magnetic fields perpendicular to the ab plane χ_{ab} and perpendicular to the c direction χ_c in four high-quality $YBa_2Cu_3O_{7-\delta}$ single crystals. Then, we compare the amplitude and the temperature behavior of these $\Delta\chi_{ab}$ and $\Delta\chi_c$ data with previous results in single-phase polycrystalline $YBa_2Cu_3O_{7-\delta}$ samples,[4,14-16] with paraconductivity data in the a direction measured in two of the samples studied in the present work, and with existing theoretical approaches.[1,2,11,23-32]

II. EXPERIMENTAL DETAILS AND RESULTS

Crystals were grown in air from CuO-BaO-rich melts by using a previously reported flux-growth technique,[33,34] slightly modified.[35] Post-annealing at 600 °C was done in order to obtain good oxygenated 90 K single crystals.[36]

The samples were examined under a polarizing optical microscope with white light, and characterized using standard single-crystal x-ray diffraction with an ENRAF-NONIUS diffractometer, model CAD4, which allows us to determine also the crystallographic axes for each sample. Most of the samples so obtained contain large untwinned domains with (110) twinned microstructure at the edges. In some cases, the untwinned region is large enough and well enough centered so it is possible to make a four electrical contact arrangement along the *a* direction with the untwinned domain between the voltage contacts (see below). This was the case of two of the samples studied here, *Ys*2 and *Ys*3 (see below). In addition, x-ray analyses show that the four samples are also single phase to better than 4%, the resolution of the measurements. Some of the general characteristics of the four samples studied here are presented in Table I.

Magnetization measurements, in low magnetic fields ($\mu_0 H \leq 0.6$ T), were made with a superconducting quantum interference device (SQUID) susceptometer (Quantum Design). The instrumental resolutions are 10^{-11} Am^2 for the magnetic moment and 0.1% for the temperature, and 10^{-5} g for the sample mass. The resolution in the magnetic susceptibility is, then, better than 5%. The samples were wrapped in a teflon strip and then rigidly held in the SQUID pickup coil's center by means of a plastic straw. The influence of the teflon strip was checked by measuring its magnetic moment under the same conditions as those of the experiment, and for $T > 70$ K it was found to be temperature independent (and of the order of -10^{-9} Am^2 for the highest fields used). This contribution was then subtracted from the magnetic moment measured for the sample with the holder. Note finally that the sample misalignment with **H** may increase the uncertainty of the data up to 10%.

Although this paper is centered on our magnetic susceptibility results, let us note here that, after the magnetic measurements were performed, a four-probe contact arrangement was made to measure the electrical resistivity in the *ab* plane. We are interested in the intrinsic OPF effects in the superconducting CuO_2 planes. So, to avoid the influence of the CuO chains that modifies the electrical resistivity in the *b* direction[6,37] in the case of the *Ys*2 and *Ys*3 samples [which have a large untwinned region in their centers (see Table I)], the electrical contacts were attached along the *a* direction, with the untwinned region between the voltage contacts. The details of these resistivity measurements will be presented elsewhere.[13] Let us stress here, however, that to avoid the influence on the ρ_a measurements of the strong anisotropy ($\rho_c \approx 10^2 \rho_a$), the electrical current contacts also covered the *cb* sample borders.

The main resistivity characteristics of the samples are presented in Table I. An example, for the sample *Ys*3, of their corresponding $\rho(T)$ curves is also presented in Fig. 1. The resistivity data of the samples *Ys*2 and *Ys*3 have been obtained in their untwinned parts, and they correspond to the *a* direction, $\rho_a(T)$. The resistivity data of the twinned *Ys*1 and *Ys*4 samples correspond to the in-plane resistivity $\rho_{ab}(T)$. In this last case, ρ_a and ρ_b will contribute to the measured resistivity, and also some contributions from the twin contacts may be present. The background resistivity, noted with the subindex *B*, corresponds to $\rho_a(T)$ and $\rho_{ab}(T)$ in the temperature region 150 K $\leq T \leq$ 250 K, and to a linear extrapolation of these resistivities for T outside this temperature region. T_{CI} is the temperature where $\rho(T)$ around the transition has its inflexion point,[4] i.e., is defined by $(d^2\rho/dT^2)_{T_{CI}} = 0$. The upper and lower half-widths, ΔT_{CI}^{+} and ΔT_{CI}^{-}, of the resistive transitions are defined by[4,13]

$$\left[\frac{d\rho(T)}{dT}\right]_{T_{CI} \pm \Delta T_{CI}^{\pm}} = \frac{1}{2}\left[\frac{d\rho(T)}{dT}\right]_{T_{CI}} . \tag{1}$$

These definitions are illustrated in Fig. 1 for the sample *Ys*3.

Concerning the $\rho(T)$ results of Table I and Fig. 1 various comments are in order. Note first that $d\rho_{abB}/dT$ (for the twinned *Ys*1 and *Ys*4 samples) is smaller than $d\rho_{aB}/dT$ (for the untwinned *Ys*2 and *Ys*3 samples), due probably to the influence of $\rho_b(T)$, which is of the order of two times smaller than $\rho_a(T)$.[6] In turn, these differences between $\rho_a(T)$ and $\rho_b(T)$ are due to the presence of the CuO chains along the *b* direction. Also, the differences for $\Delta T_{CI}^{\pm}$ between the untwinned and the twinned samples are not significant. This result suggests that $\Delta T_{CI}^{\pm}$ will mainly depend on the stoichiometric characteristic of the samples, and that they are not very sensitive to the presence of the twin boundaries. In any

TABLE I. General characteristics of the $YBa_2Cu_3O_{7-\delta}$ single crystals measured in this work. The resistivity data of samples *Ys*2 and *Ys*3 have been obtained in their untwinned part and they correspond to the *a* direction, ρ_a. The resistivity data of the twinned *Ys*1 and *Ys*4 samples correspond to the in-plane resistivity, ρ_{ab}. The background resistivity, noted with subindex *B*, corresponds to ρ_a or ρ_{ab} in the temperature region 150 K $\leq T \leq$ 250 K, and to a linear extrapolation of these resistivities outside this temperature region. The other quantities are defined in the main text.

Crystal	Dimensions (mm^3)	Mass (mg)	Untwinned ($a \times b$) region (mm^2)	$\rho_B(0)$ ($\mu\Omega$ cm)	$d\rho_B/dT$ ($\mu\Omega$ cm K^{-1})	T_{CI} (K)	ΔT_{CI}^{+} (K)	ΔT_{CI}^{-} (K)	$T_{C\chi}$ (K)
*Ys*1	1.75×1.3×0.06	0.90	non	0.0	0.50	89.00	0.20	0.15	89.0
*Ys*2	2.25×1.2×0.07	1.20	0.3×1.2	−1.0	0.72	90.05	0.15	0.10	90.0
*Ys*3	1.60×0.5×0.07	0.50	0.5×0.5	3.0	0.75	90.80	0.10	0.05	90.8
*Ys*4	2.10×1.1×0.08	1.17	non	1.5	0.65	90.30	0.15	0.15	90.4

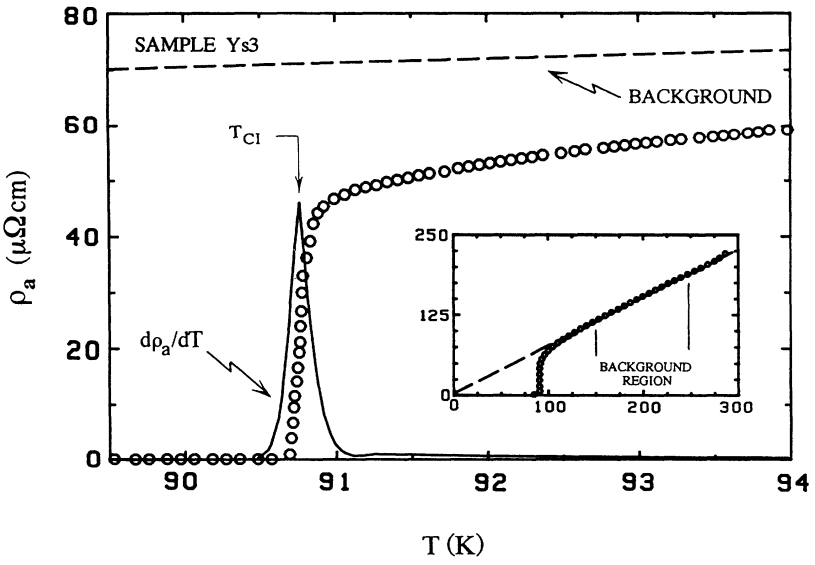

FIG. 1. Detailed view around the transition of the in-plane longitudinal resistivity along the *a* axis of sample *Ys*3. The inset shows an extended view of the in-plane longitudinal resistivity along the *a* axis of sample *Ys*3. The dashed line is the so-called background resistivity obtained by fitting in the indicated background region.

case, these $\Delta T_{CI}^{\pm}$ values are, for the four samples studied here, exceptionally small, providing then a further indication of the excellent stoichiometric homogeneity of these samples. This last conclusion is also confirmed by our magnetic measurements (see below): $\chi_{ab}(T)$ in the background region, and $\chi_c(T)$ all above the superconducting transition are found to be almost temperature independent, showing then the absence of important paramagnetic contributions (due, for instance, to impurities or oxygen disorder). Note, finally, that for each one of the samples, T_{CI} agrees within ΔT_{CI}^{+} with $T_{C\chi}$, the temperature where $\chi_c(T)$ [and $\chi_{ab}(T)$, see later] goes through zero. This result will justify the use of $T_{C\chi}$ as T_{CO} (see below).

Figure 2 shows the temperature dependence of χ_{ab}, the magnetic susceptibility (in MKS units) for sample *Ys*3, with $T_{C\chi}=90.8$ K. As noted before, $T_{C\chi}$ is defined $\chi_c(T_{C\chi})=0$, but for all the samples studied here it agrees, to within the experimental uncertainties, with the temperature where $\chi_{ab}(T)$ goes also through zero. [This last result justifies, therefore, our earlier proposal that it is a reasonable approximation to use $\chi(T_{CO})=0$ to obtain T_{CO} also in single-phase polycrystalline samples.[4]] Both zero-field-cooled (ZFC) and field-cooled (FC) measurements were made with the applied magnetic field ($\mu_0 H=5$ mT) perpendicular to the *ab* plane. For temperatures well below $T_{C\chi}$, where the value of the magnetic moment is large, the effect of the demagnetization field must be taken into account, because the value of the internal field, H_i, may be much bigger than H. In the simplest case of a uniformly magnetized system, and for H applied along a principal axis, $H_i=H-DM$, where D is the demagnetization factor and M is the magnetization (magnetic moment per unit volume). The sample volume is determined from its mass by using the theoretical density of the $YBa_2Cu_3O_7$ (6.32 g/cm^3). To estimate D, we have used the ellipsoidal approximation, and then, compared its value with the one obtained by assuming a fully diamagnetic signal at the lowest temperature ($T=5$ K), i.e., $\chi=-1$, where $\chi=M/H_i$. For this sample, a value of 0.95 has been estimated as demagnetization factor. With it, this sample shows 97% of diamagnetic screening and about 20% of flux expulsion. This general behavior of $\chi_{ab}(T)$ agrees with those obtained in the best single crystals measured until now.[36]

Above the superconducting transition, the intrinsic susceptibility of $YBa_2Cu_3O_{7-\delta}$ is very small, of the order of (in MKS units) 5×10^{-5} and 2.5×10^{-5} for the field perpendicular and parallel to the *ab* plane, respectively (see below). So, although the OPF effects just above the transition will appreciably modify $\chi_{ab}(T)$, to resolve the variations of such a small magnetic susceptibility we must increase the resolution of Fig. 2 by at least a factor of 10^5. For that we restrict the measurements to the region where $\chi_{ab}(T)$ is positive, and they are performed under applied magnetic fields of the order of one hundred times bigger than those of Fig. 2, i.e., between 0.2 T and 0.6 T. To check that these magnetic fields parallel to the

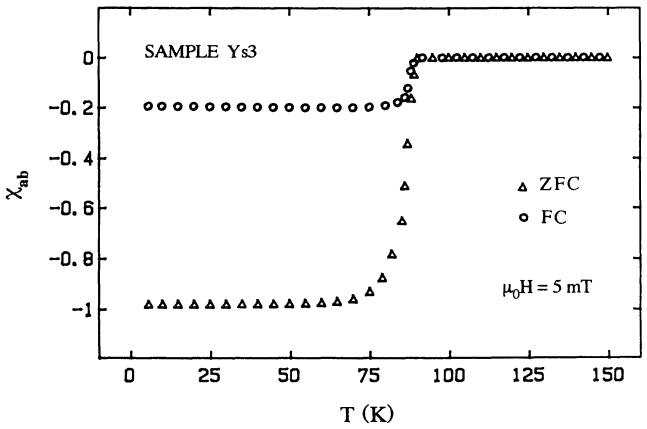

FIG. 2. Temperature dependence of the magnetic susceptibility χ_{ab} for sample *Ys*3, measured with $\mu_0 H=5$ mT perpendicular to the *ab* plane. Triangles and circles correspond to ZFC and FC measurements, respectively.

c axis do not modify, at least in the mean-field-like region (MFR), the OPF effects in the ab plane, and that these effects may still be estimated by using the Gaussian approximations for independent fluctuations of each order parameter component, we may use the criterion that these approximations remain valid if[20]

$$l_H \equiv \left[\frac{\hbar}{2e\mu_0 H}\right]^{1/2} \gg \xi_{ab}(\varepsilon) , \tag{2}$$

where l_H is the so-called magnetic length, e is the electron charge, $\hbar$ is the reduced Planck constant,

$$\xi_{ab}(\varepsilon)=\xi_{ab}(0)\varepsilon^{-1/2} \tag{3}$$

is the superconducting correlation length in the ab plane,

$$\varepsilon \equiv \ln\frac{T}{T_{CO}} \approx \frac{T-T_{CO}}{T_{CO}} \tag{4}$$

is the reduced temperature, and T_{CO} is the mean-field transition temperature. By combining Eqs. (2)–(4), the above condition may be rewritten as

$$\varepsilon \gg \frac{2\pi\mu_0 H\xi_{ab}^2(0)}{\phi_0} = \frac{H}{H_{c2}^{\parallel c}(0)} , \tag{5}$$

where $\phi_0=h/2e$ is the flux quantum and $H_{c2}^{\parallel c}(0)$ is the amplitude (for $T=0$) of the upper critical magnetic field parallel to the c direction (see below). For $\mu_0 H=0.6$ T, and if, for instance, $\xi_{ab}(0)\approx 1.1$ nm, deviations to the zero-field OPF behavior may be expected if $\varepsilon \lesssim 2\times 10^{-3}$. This last reduced temperature is less than the expected Ginzburg temperature (see later) and, therefore, we may expect that for $\mu_0 H \lesssim 0.6$ T the OPF effects are not modified by the applied magnetic field in all the MFR. These conclusions are confirmed by the results of Fig. 3, where we show the magnetization, for sample $Ys3$, around the transition and measured with $\mu_0 H=0.4$ T (circles) and $\mu_0 H=0.6$ T (triangles), both perpendicular to the ab plane. These data were corrected for a small Curie-Weiss-like contribution. The dashed lines represent the extrapolation through the superconducting transition of the normal-state data between $T_{C\chi}+60$ K and $T_{C\chi}+160$ K.[4] As it can be easily seen, the susceptibilities that may be extracted from each curve by just dividing by the corresponding magnetic field are the same within the experimental resolution, and this is true in all the rounded region above the transition. These results confirm that our present measurements verify Eq. (2). [Note also that $T_{C\chi}$, the temperature where $M(T)$ goes through zero, and that were are going to approximate as the mean-field critical temperature (see later), is not appreciably affected, independently of the H direction in relation to the layers, by these low magnetic fields.] This last result is also in agreement with the magnetic-field dependence of the mean-field critical temperature predicted by the Abrikosov-Gorkov (AG) theory.[38,39] In layered superconductors and for H perpendicular to the layers, the AG theory leads to[13]

$$\ln\frac{T_{CO}(0)}{T_{CO}(H)} = \xi_{ab}^2(0) l_H^{-2} . \tag{6}$$

For $\mu_0 H=0.6$ T and $T_{CO}=90$ K, and by using again $\xi_{ab}(0)=1.1$ nm, we found $T_{CO}(0)-T_{CO}(H)\approx 0.15$ K, which is a bit higher than the instrumental temperature resolution. The values of $T_{C\chi}$ for the four samples studied here are given in the last column of Table I, and they have been corrected of the corresponding magnetic-field-induced temperature shift. Note also that the values of $T_{C\chi}$ defined, as noted before, by $\chi_{ab}(T_{C\chi})=0$ agree within $\Delta T_{CI}(\approx 0.25$ K) with T_{CI}, obtained for each samples from the $\rho(T)$ data in zero applied magnetic field as indicated above. The values of $T_{C\chi}$ are indicated for samples $Ys3$ in Figs. 3 and 4(b). So, in the remainder of our paper we will use $T_{C\chi}$ or T_{CI} as mean-field-like critical temperature (see below).

The magnetic susceptibility of sample $Ys3$ measured with the magnetic field applied perpendicular to the ab plane χ_{ab} (open symbols) and parallel to the ab plane χ_c (solid symbols) is shown in Fig. 4(a). The dashed lines represent the constant normal-state background for both field orientations χ_{abB} and χ_{cB}, respectively. We find $\chi_{abB}\approx 5.2\times 10^{-5}$ and $\chi_{cB}\approx 2.7\times 10^{-5}$. These values for the susceptibility in the normal region are relatively similar (to within 20%) to those obtained in other measurements in single crystals,[18,19,40] or in single-phase aligned powder[16] or ceramic samples.[41] It is interesting to remark that these experimental values of χ_{abB} and χ_{cB} are also reasonably close to those calculated in Ref. 42 by the spin density functional-random phase (SDFA-RPA) approach (4.4×10^{-5} and 3.5×10^{-5} for χ_{abB} and χ_{cB}, respectively). Note also that just above $T_{C\chi}$, $\chi_{ab}(T)$ is appreciably rounded, i.e., $\chi_{ab}(T)$ decreases below $\chi_{abB}(T)$ well above $T_{C\chi}$. This is clearly showed by the results of Fig. 4(b). In contrast, $\chi_c(T)$ remains almost constant and similar to $\chi_{cB}(T)$ even close but above $T_{C\chi}$. In the next section we will see that these behaviors above but near $T_{C\chi}$ may be explained using the existing approaches for OPF effects on $\chi(T)$ in layered superconductors.[1,2,23–26,32] Note also that the results of Fig. 4(a)

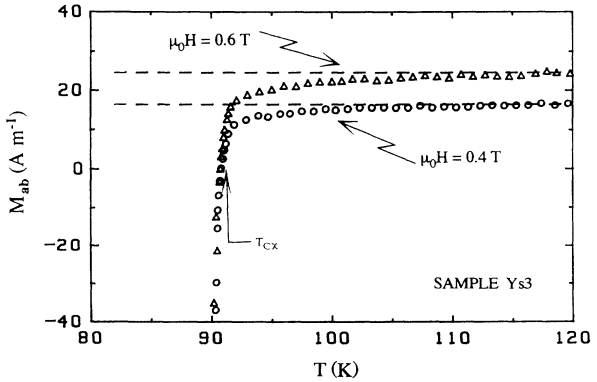

FIG. 3. Magnetization data for sample $Ys3$ measured with $\mu_0 H=0.4$ T (circles) and $\mu_0 H=0.6$ T (triangles), both perpendicular to the ab plane. The dashed lines are the corresponding backgrounds. $T_{C\chi}$ is the temperature for which $M_{ab}(T)$ goes through zero. For clarity only about 20% of the data points obtained have been plotted.

clearly indicate that above $T-T_{C\chi}\approx 25$ K, i.e., for $\varepsilon \gtrsim 0.3$, $\chi_{ab}(T)$ becomes independent of T in all the temperature range where the present measurements have been performed. In other words, our susceptibility measurements in weak magnetic fields clearly confirm our previous paraconductivity data suggesting that the amplitude of the possible OPF effects for $\varepsilon \gtrsim 0.3$ becomes smaller than the accuracy of the measurements of the different observables studied (see also next section).

The results of Fig. 4(a) also show that the temperatures where χ_{ab} or χ_c go through zero agree to each other. This temperature is noted $T_{C\chi}$ and, as noted before, also agrees to within ΔT_{CI} with T_{CI}. As for H perpendicular to the c direction, the OPF influence on $\chi_c(T)$ is expected to be negligible, these results confirm our earlier proposal[4] that it is reasonable the use of $T_{C\chi}$ or of T_{CI} as T_{CO}, the mean-field-like critical temperature, in all the measurements in the weak magnetic-field limit defined by Eq. (2). Finally, let us note that the magnetic susceptibilities

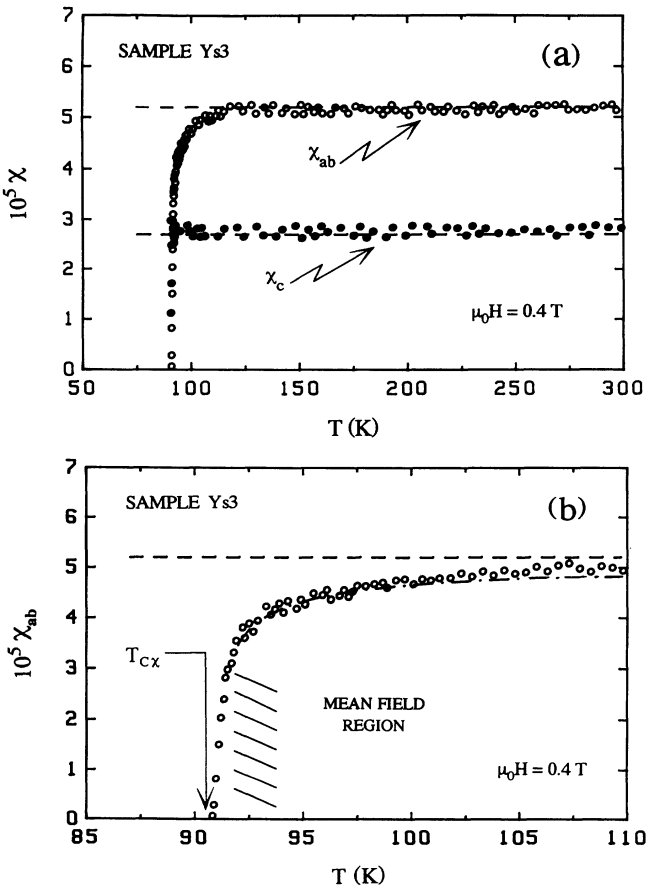

FIG. 4. (a) Temperature behavior of the magnetic susceptibility of sample $Ys3$ for $\mu_0 H = 0.4$ T, with H perpendicular (open circles) and parallel (solid circles) to the ab plane. The dashed lines are the normal-state background susceptibilities. (b) Temperature dependence of the magnetic susceptibility for H perpendicular to the ab plane around the transition. The dashed line is the normal-state background susceptibility extrapolation through the transition. The dot-dashed line is the mean-field-like prediction in the indicated mean-field region.

of the four samples studied here agree, to within the measurement resolution, with each other. Such an agreement just indicates then that the presence of twins seems not to modify appreciably the magnetic susceptibility in all the studied temperature range, including the region affected by OPF effects (see below). Note also that as the untwinned region of samples $Ys2$ and $Ys3$ is only about 30% of their total surface, we are not able to discriminate between χ_c with H parallel to the a or b direction.

III. FLUCTUATION-INDUCED DIAMAGNETISM ABOVE THE SUPERCONDUCTING TRANSITION

The fluctuation-induced diamagnetism, also called "excess" diamagnetism, for the magnetic field applied perpendicular or parallel to the ab planes and noted, respectively, $\Delta\chi_{ab}$ and $\Delta\chi_c$, are defined by

$$\Delta\chi_{ab}(\varepsilon) \equiv \chi_{abB}(\varepsilon) - \chi_{ab}(\varepsilon) , \tag{7}$$

and

$$\Delta\chi_c(\varepsilon) \equiv \chi_{cB}(\varepsilon) - \chi_c(\varepsilon), \tag{8}$$

where the terms noted with the subindex B are the so-called "bare" or background" contributions, and they are expected to be rather insensitive to the presence of the transition. The theoretical treatments that we are going to use in the next section apply to the "excess" contribution to each measured observable. As a consequence, we must stress here for $\Delta\chi$, as we have already done for the paraconductivity,[13,43,44] and for the thermoelectric power,[45] that a meaningful comparison between the theories and the experimental results is possible only if the background part can be estimated *independently*, the existing theoretical formalism being unable to allow for these short-wavelength fluctuations. In doing that, the fundamental and general assumption used is that such a background remains finite at the critical point if it is finite elsewhere. A quantitative estimation of the background terms needs, however, the help of other conjectures which will depend on each property studied. In general, one looks for any functional form, provided or not by the theory of the normal state, that fits closely the normal-state temperature trend over a wide temperature region far away from the transition, and that extrapolates smoothly through the transition. For the background susceptibility with H parallel or perpendicular to the ab plane $\chi_{cB}(T)$ or, respectively, $\chi_{abB}(T)$, we use the extrapolation of $\chi_c(T)$ and $\chi_{ab}(T)$ measured in the temperature region bounded by $150\ \text{K} \le T \le 250$ K, a region where the influence of the OPF effects on any magnitude is expected to be negligible.[1,2,20,45] Indeed, this background choice is a source of uncertainty unless a functional form for the normal-state temperature dependence and amplitude of the measured magnitude is firmly established. However, the fact that, in agreement with the existing theoretical estimations,[42] χ_{ab} and χ_c are found to be temperature independent for $T-T_{C\chi} \gtrsim 25$ K and up to $T = 300$ K, the highest temperature studied here, mitigates somewhat these uncertainties. So, the modification proposed in other works[16,24] of the background estimated in the present work could lead to the unreasonable con-

clusion of the existence of appreciable OPF effects even at more than 200 K above the transition. Furthermore, as we already stressed in the case of the paraconductivity,[43,44] it must be obvious that with a free background almost any theoretical excess diamagnetism may fit reasonably well the experimental data in any ε region. This will, therefore, prevent any discrimination among the different theoretical explanations of the rounding effects on $\chi(T)$ above T_{CO} in high-temperature superconductors.

In Fig. 5(a) we compare $\Delta\chi_{ab}(\varepsilon)$ and $\Delta\chi_c(\varepsilon)$ for sample *Ys*3. From this figure it can be seen that the OPF influence on $\chi_c(\varepsilon)$ is negligible. In Fig. 5(b) we show $\Delta\chi_{ab}(\varepsilon)$ for sample *Ys*3, obtained with $\mu_0 H = 0.4$ T (circles) and with $\mu_0 H = 0.6$ T (triangles). These data agree to each other to within the experimental dispersion, confirming then that they do not depend on H, i.e., that these $\Delta\chi_{ab}(\varepsilon)$ data correspond to the zero magnetic-field limit. In Fig. 6 we present the $\Delta\chi_{ab}(\varepsilon)$ data obtained from two of the single-crystal samples studied here, one of them having a large untwinned region in its center. The results for the other two samples studied here are well inside the data dispersion of this figure. The good agreement between all these results for the four different samples strongly suggests that these data are not appreciably affected by possible nonintrinsic effects, as those due to the demagnetization factors (the samples have different shapes) or the presence of twin lines. We may conclude, therefore, that the results of Figs. 5 and 6 are the intrinsic fluctuation-induced diamagnetism of $YBa_2Cu_3O_{7-\delta}$ compounds, above the superconducting transition.

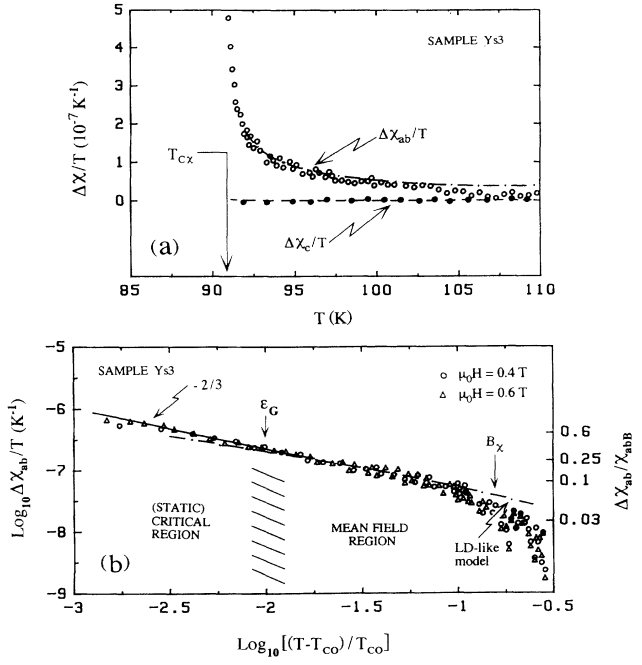

FIG. 5. (a) Excess diamagnetism (over T) versus temperature for sample *Ys*3 measured with $\mu_0 H = 0.4$ T perpendicular (open circles) and parallel (solid circles) to the *ab* plane. The dashed line was obtained by multiplying the dot-dashed line by the constant factor $[\xi_c(0)/\xi_{ab}(0)]^2$ with $\xi_{ab}(0) = 1.1$ nm and $\xi_c(0) = 0.12$ nm. (b) Log-log plot of the excess diamagnetism (over T) versus reduced temperature, measured with the applied magnetic field perpendicular to the *ab* plane for sample *Ys*3 with $\mu_0 H = 0.4$ T (circles) and $\mu_0 H = 0.6$ T (triangles). The solid line is the scaling prediction beyond the MFR, in the so-called static critical region. In these figures the dot-dashed lines are the best fit of the extension to layered superconductors of the Schmidt approaches for the fluctuation-induced diamagnetism.

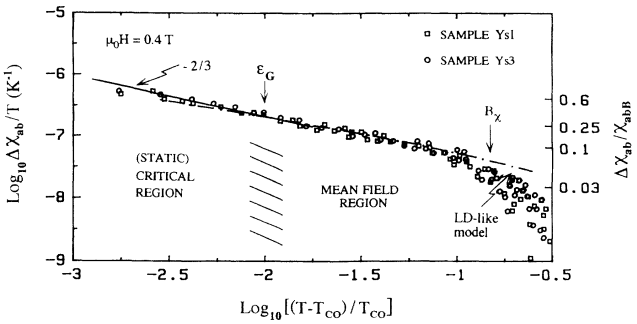

FIG. 6. Log-log plot of the excess diamagnetism (over T) versus reduced temperature for sample *Ys*1 (squares) and sample *Ys*3 (circles) with $\mu_0 H = 0.4$ T. The results for the other two samples studied here are well inside the data dispersion of this figure. The solid line is the scaling prediction beyond the MFR, in the so-called static critical region. In this figure the dot-dashed line is the best fit of the extension to layered superconductors of the Schmidt approaches for the fluctuation-induced diamagnetism.

The results of Figs. 5 and 6 agree qualitatively with those that we have extracted previously from measurements in polycrystalline $YBa_2Cu_3O_{7-\delta}$ bulk samples, by assuming that the corresponding structural inhomogeneities mainly were at long length scales, i.e., at length scales much larger than any characteristic length relevant for OPF effects, as for instance the superconducting correlation length in all directions, and that the *ab* planes of the different sample domains are randomly oriented.[4] The good agreement with the present $\chi_{ab}(\varepsilon)$ data, obtained in single crystals, is a nice indication of the correctness of such an approximation. Concerning the $\Delta\chi_{ab}(T)$ data from other groups, our values agree qualitatively with those obtained in single crystals[18,19] or in polycrystal samples,[15] although these last results

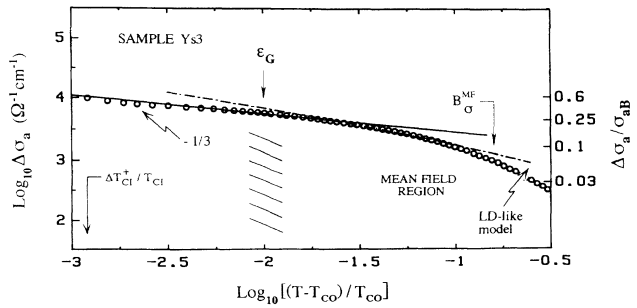

FIG. 7. Paraconductivity along the *a* axis of sample *Ys*3 versus reduced temperature. The dot-dashed line corresponds to the Lawrence-Doniach extensions to layered materials of the Aslamazov-Larkin results for the fluctuation-induced conductivity and the solid line is the dynamic scaling prediction for the (full) critical region of the 3D XY model.

penetrate only up to $\varepsilon \approx 5\times10^{-2}$ above $T_{C\chi}$. In contrast, the $\Delta\chi_{ab}(T)$ data proposed in Ref. 16, obtained from measurements in grain-aligned polycrystal samples, are approximately 50% higher than our data, despite that their values of $\chi_{ab}(T)$ are similar to ours (within 20%). These differences were already observed in the comparison of the $\Delta\chi_{ab}(T)$ data of Ref. 16 with our results in single-phase polycrystal samples, as can be seen in Fig. 2(b) of Ref. 4. So, they are not due to the polycrystallinity of the samples of Ref. 16. Probably these differences in amplitude are mainly associated with the background subtraction procedure followed by those authors.

For completeness, in Fig. 7 we present the excess (or para-) conductivity in the *a* direction $\Delta\sigma_a$ of sample *Ys*3. These data were extracted from the $\rho_a(T)$ data, not affected by the presence of CuO chains, following the same procedure as indicated in Refs. 4 and 13, and their corresponding errors, which as indicated before are mainly due to geometrical uncertainties, are of the order of 15%. Note that the ε behavior of $\Delta\sigma_a(\varepsilon)$ in Fig. 7 agrees fairly well with that of $\Delta\sigma_{ab}(\varepsilon)$, the paraconductivity in the *ab* plane that we have extracted before from measurements in *single-phase* polycrystalline $YBa_2Cu_3O_{7-\delta}$ samples,[4,22,45] the influence of the structural inhomogeneities at long length scales being taken into account through the empirical picture described in Refs. 4 and 45 and in the references therein. [So, as noted in Ref. 4, no fractal effects arise on $\Delta\sigma_{ab}(\varepsilon)$ in single-phase polycrystalline samples.] However, as $d\rho_a(T)/dT$ is of the order of 25% bigger than $d\rho_{ab}(T)/dT$, the same differences are found between the $\Delta\sigma_a$ (the *intrinsic* paraconductivity) and $\Delta\sigma_{ab}$ (affected by the CuO chains) *amplitudes*.

The data of Figs. 5(a), 5(b), and 6 are the central results of this paper, because they provide information, with high amplitude and temperature resolution, of both $\Delta\chi_{ab}(\varepsilon)$ and $\Delta\chi_c(\varepsilon)$ of good $YBa_2Cu_3O_{7-\delta}$ single crystals. Let us already stress that the comparison of $\Delta\chi_{ab}(\varepsilon)/T$ (Fig. 5) with $\Delta\sigma_a(\varepsilon)$ (Fig. 7) for sample *Ys*3 confirms that, as noted in Ref. 4, both magnitudes have the same ε behavior for $\varepsilon \gtrsim 10^{-2}$, a region of temperatures that corresponds to the so-called mean-field region (see next section). To check quantitatively this result, in Fig. 8 we represent $\Delta\chi_{ab}(\varepsilon)/\Delta\sigma_a(\varepsilon)T$ obtained by using directly the experimental data of Figs. 5 and 7. The results of Fig. 8 fully confirm at a quantitative level our previous results obtained in single-phase polycrystalline samples, and they suggest that any possible pair-breaking (Maki-Thompson) effect having the proposed behavior[27,46–49] will contribute by less than 20% to the measured $\Delta\sigma_a(\varepsilon)$ amplitude in all the examined ε range. The corresponding phase-relaxation time in the clean limit,[27,47–49] $\tau_{\phi c}$, will be for $YBa_2Cu_3O_{7-\delta}$ compounds less than 5×10^{-15} s. Note that the theoretical analysis of the absence or not of an appreciable pair-breaking contribution to $\Delta\sigma_{ab}(\varepsilon)$ in $YBa_2Cu_3O_{7-\delta}$ compounds is still controversial,[27,31,46–49] and we cannot exclude the presence of a Maki-Thompson term in $\Delta\sigma_{ab}$ with similar ε dependence than the Aslamazov-Larkin term. However, we will see in the next section that our analysis of the $\Delta\chi_{ab}(\varepsilon)$ and $\Delta\sigma_a(\varepsilon)$ *amplitudes* also suggests a negligible pair-breaking contribution to $\Delta\sigma_a(\varepsilon)$, and that, in this case, the relationship $\Delta\chi_{ab}(\varepsilon)/\Delta\sigma_a(\varepsilon)T$ also allows a direct estimation of $\xi_{ab}(0)$, the Ginzburg-Landau (mean-field) order parameter correlation length amplitude (at $T=0$ K) in the *ab* plane. The results of Fig. 8 also show that for $\varepsilon \lesssim 10^{-2}$, $\Delta\chi_{ab}(\varepsilon)/\Delta\sigma_a(\varepsilon)T$ depends on ε. We will see in the next section that such a dependence may be explained by assuming that below $\varepsilon \lesssim 10^{-2}$ the (full) critical region is penetrated. However, we must stress that so close to T_{CO} the presence of small inhomogeneities may appreciably affect both $\Delta\chi_{ab}(\varepsilon)$ and $\Delta\sigma_a(\varepsilon)$.

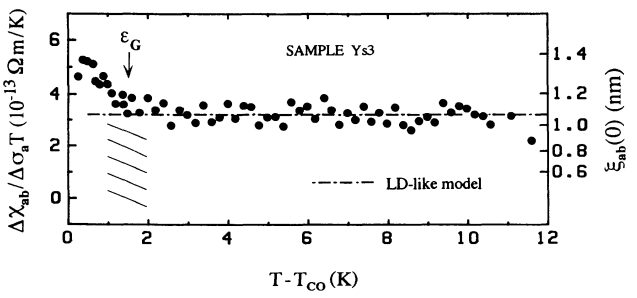

FIG. 8. Relationship between the excess diamagnetism over T for H applied perpendicular to the *ab* plane and the excess conductivity in the *a* direction for sample *Ys*3 in the mean-field-like region. The dot-dashed line corresponds to the theoretical prediction for the OPF in the mean-field-like region [Eq.(16)], with $\xi_{ab}(0)=1.1$ mm.

IV. COMPARISON WITH THEORETICAL APPROACHES IN THE WEAK MAGNETIC-FIELD LIMIT

We are now able to compare our excess diamagnetism results with the existing theoretical approaches for $\Delta\chi_{ab}(\varepsilon)$ in the mean-field-like region (MFR) and in the weak applied magnetic-field limit $[l_H \gg \xi_{ab}(\varepsilon)]$.[11,23–32] By assuming already a complex order parameter with two real components[4,12,13,23,28] and two CuO_2 superconducting planes by unit cell,[23,27,30,32] the existing theoretical results for $\Delta\chi_{ab}(\varepsilon)$ and $\Delta\sigma_a(\varepsilon)$ may be summarized as[11,23–32]

$$\Delta\sigma_a(\varepsilon)=\frac{A_\sigma}{\varepsilon}\left[1+\frac{B_\sigma}{\varepsilon}\right]^{-1/2} \tag{9}$$

and

$$\Delta\chi_{ab}(\varepsilon)/T=\frac{A_\chi}{\varepsilon}\left[1+\frac{B_\chi}{\varepsilon}\right]^{-1/2}, \tag{10}$$

where

$$A_\sigma \equiv \frac{e^2}{8\hbar s} \tag{11}$$

and

$$A_\chi \equiv \frac{2\mu_0\pi k_B \xi_{ab}^2(0)}{3\phi_0^2 s}, \tag{12}$$

are twice the Aslamazov-Larkin conductivity and the

Schmidt diamagnetism (over T), respectively, k_B is the Boltzmann constant,

$$B_{\sigma,\chi} \equiv \left[\frac{4\xi_c(0)}{s} \right]^2 \tag{13}$$

is the parameter that controls the two-dimensional-three-dimensional (2D-3D) crossover of the dimensionality of the OPF in the MFR, $\xi_c(0)$ is the amplitude (at $T=0$ K) of the order parameter correlation length in c direction, and s is the unit-cell length. In these expressions ε is given by Eq. (4), and for T_{CO} we will use $T_{C\chi}$ for H parallel to the ab plane, as defined before. Note that in these expressions we have assumed the same Josephson coupling strength for the *two* CuO_2 layers in s, the unit-cell length.[12,23,32] This is equivalent to using $s/2$ instead of s in the conventional Lawrence-Doniach (LD)-like approaches for one superconducting layer per unit-cell length.[16,32]

The above results apply in the mean-field region (MFR), i.e., in the reduced temperature range where the time-dependent Ginzburg-Landau (TDGL)-like approaches, and the Gaussian approximations for OPF in the weak magnetic-field limit, are expected to be applicable without taking into account local and high-temperature effects.[1,2,11,23–32,48,49] The lower ε limit of the MFR is associated with the so-called Ginzburg reduced temperature ε_G. For OPF in three dimensions (3D), the case which is expected to hold for $YBa_2Cu_3O_{7-\delta}$ superconductors,[4,22] and for $H \rightarrow 0$, is given by[2]

$$\varepsilon_G = \frac{1}{32\pi^2} \left[\frac{k_B}{\xi_{ab}^2(0)\xi_c(0)\Delta C} \right]^2 . \tag{14}$$

Here, ΔC is the specific-heat jump at the transition. By using for the $YBa_2Cu_3O_{7-\delta}$ system (see below), $\xi_{ab}(0) \approx 1.1$ nm, $\xi_c(0) \approx 0.12$ nm, and[50,51] $\Delta C \approx 3.6 \times 10^4$ J m^{-3}K^{-1}, we obtain $\varepsilon_G \approx 10^{-2}$. Note also that these ε_G values agree with the lower ε limit where Eqs. (9) and (10) fit well (with a rms deviation of 3–10 %) our experimental $\Delta\sigma_a(\varepsilon)$ and $\Delta\chi_{ab}(\varepsilon)$ results (see below). For $\varepsilon \gtrsim 0.15$, not only the slow variation condition of the TDGL-like theories will probably fail,[20,23] but also any calculation of the OPF effects cannot be trusted unless it takes full account of the dynamic local effects.[1,11,20,23–32,48,49] In addition, by using $\xi_c(0) \approx 0.12$ nm, we see that for $\varepsilon \gtrsim 0.15$, $\xi_c(\varepsilon)$ will become even smaller than the interatomic distances. Also, so far from the transition, the experimental uncertainties in $\Delta\chi_{ab}(\varepsilon)$ become even bigger than the average measured $\Delta\chi_{ab}(\varepsilon)$. Therefore, for $\varepsilon \gtrsim 0.15$, the conventional MFR approach to layered superconductors is probably no longer applicable (see below).

Some general aspects of Eqs. (9) and (10) for $\Delta\sigma_a(\varepsilon)$ and for $\Delta\chi_{ab}(\varepsilon)$ in the MFR must be commented upon here.

(i) In these expressions we have neglected the possible small terms proportional to $[\xi_c(0)/\xi_{ab}(0)]^2$. The correctness for the $YBa_2Cu_3O_{7-\delta}$ system of this last approximation is supported by the comparison between our experimental results for $\Delta\chi_c(\varepsilon)$ and the corresponding theoretical approach: In the MFR, $\Delta\chi_c(\varepsilon)$ is given by[23,32]

$$\Delta\chi_c(\varepsilon) \approx \left[\frac{\xi_c(0)}{\xi_{ab}(0)} \right]^2 \Delta\chi_{ab}(\varepsilon) , \tag{15}$$

and the results of Fig. 5(a) clearly show that $\Delta\chi_c(\varepsilon) \ll \Delta\chi_{ab}(\varepsilon)$. In this figure, the dashed line is obtained by using in Eq. (15), $\xi_{ab}(0)=1.1$ nm, and $\xi_c(0)=0.12$ nm, and for $\Delta\chi_{ab}(\varepsilon)$ the experimental results given in the same figure.

(ii) From Eqs. (9)–(12), we obtain (in MKS units)

$$\frac{\Delta\chi_{ab}(\varepsilon)/T}{\Delta\sigma_a(\varepsilon)} = 2.79 \times 10^5 \xi_{ab}^2(0) , \tag{16}$$

a relationship that, in full agreement with the result of Fig. 8, is ε independent. Indeed, in this equation $\Delta\sigma_a(\varepsilon)$ is assumed to be due only to direct OPF effects. This last result confirms, then, that both the measured excess conductivity and diamagnetism in the ab plane are probably due to direct OPF effects. In addition, Eq. (16) allows a straight estimation of $\xi_{ab}(0)$. By combining the results of Fig. 8 with Eq. (16), we obtain

$$\xi_{ab}(0) = (1.1 \pm 0.2) \text{ nm} , \tag{17}$$

in agreement with our previous results obtained in *single-phase* polycrystalline $YBa_2Cu_3O_{7-\delta}$ samples.[4] The uncertainties of Eq. (17) take into account the errors in both $\Delta\chi_{ab}(\varepsilon)$ and $\Delta\sigma_a(\varepsilon)$, this last observable being extracted from our resistivity data in sample *Ys*3. The values of $\xi_{ab}(0)$ obtained following the same procedure for the three other samples studied here are within the experimental error of Eq. (17). In our previous analysis,[4] this value of $\xi_{ab}(0)$ was discarded because it was considered too low when compared with the average values proposed in the literature,[52] $\xi_{ab}(0)=(1.4\pm0.2)$ nm. (See, also, scenario B in Table I of Ref. 12.) Also, from previous $\Delta\chi(\varepsilon)$ results in bulk polycrystals and films, it was proposed [16] $\xi_{ab}(0) \approx 1.4$ nm. However, recent analyses of the $dH_{C2}(T)/dT$ measurements, from which independent $\xi_{ab}(0)$ values may be obtained, seem to indicate that the value of $\xi_{ab}(0)$ given by Eq. (17) cannot be ruled out.[53] In fact, our preliminary measurements of $dH_{C2}(T)/dT$ and of $T_{C\chi}(H)$ or $T_{CI}(H)$ in the four samples studied here are compatible, when analyzed in terms of the Ginzburg-Landau approach and, respectively, of the Abrikosov-Gorkov approach, with the $\xi_{ab}(0)$ value of Eq. (17). The

TABLE II. Experimental values of the parameters arising in the Lawrence-Doniach-like descriptions of the fluctuation-induced diamagnetism above the superconducting transition in the $YBa_2Cu_3O_{7-\delta}$ single crystals studied here.

Sample	Fitting region ε^{low}	ε^{up}	rms deviation	A_χ (10^{-9} K^{-1})	B_χ
*Ys*1	1.5×10^{-2}	10^{-1}	8%	6.4±1.5	0.12±0.02
*Ys*2	3×10^{-2}	1.5×10^{-1}	8%	7.5±1.5	0.14±0.03
*Ys*3	2×10^{-2}	10^{-1}	10%	8.7±1.8	0.17±0.03
*Ys*4	1.5×10^{-2}	1.5×10^{-1}	9%	10.8±2.0	0.18±0.03

remaining differences among the various values of $\xi_{ab}(0)$ could be due to the fact that $dH_{C2}(T)/dT$ is not measured in the $l_H \gg \xi_{ab}(\varepsilon)$ limit and to the moving vortex lines below T_{CO}.

We may now obtain the values of $\xi_c(0)$ by just fitting Eq. (10) to the experimental $\Delta\chi_{ab}(\varepsilon)$ data, with A_χ and B_χ as free parameters. The dot-dashed curves in Figs. 4(b), 5(a), 5(b), and 6 are examples of the resulting curves. The fitting regions for the different samples are indicated in Table II, where we present also the resulting A_χ and B_χ parameters. The values of $\xi_c(0)$, obtained from the B_χ values of Table II through Eq. (13), are within

$$\xi_c(0)=(0.12\pm0.02)\ \text{nm} \ . \tag{18}$$

As noted in the Introduction, this paper is focused on the OPF effects on the magnetic susceptibility in the so-called mean-field-like region above the transition, i.e., on the ε region where the extensions to layered materials of the conventional (time-dependent, in the case of σ) Ginzburg-Landau approaches, without local or high-temperature corrections, are expected to be applicable. However, as the temperature resolution of our $\chi(T)$ measurements is of the order of 0.1 K, we were able to penetrate somewhat beyond our estimated ε_G, in the so-called static (critical) region, as shown in Figs. 5(b), 6, and 7. These $\Delta\chi_{ab}(\varepsilon)$ and $\Delta\sigma_a(\varepsilon)$ data in an ε region so close to the transition may be strongly affected by the presence of small stoichiometric inhomogeneities (oxygen content, for instance).[54] Also, in that ε region the reduced temperature uncertainties are relatively important. However, the results of Fig. 8 of $\Delta\chi_{ab}(\varepsilon)/\Delta\sigma_a(\varepsilon)T$ for sample *Ys*3 clearly confirm that for $T-T_{CO}\lesssim 2$ K the experimental data separate from the temperature independent behavior predicted for the MFR by the LD-like approaches [Eq. (16)]. Note also that for $\varepsilon\lesssim 10^{-2}$, $\Delta\chi_{ab}(\varepsilon)/\chi_{abB}(\varepsilon)\gtrsim 0.3$. This is a very direct indication that for $\varepsilon\lesssim 10^{-2}$ the contributions associated with the fluctuations are no longer a small correction to the background behavior. These results fully confirm our early measurements of $\Delta\chi(\varepsilon)$ [and of $\Delta\sigma(\varepsilon)$] for $\varepsilon\lesssim 10^{-2}$ in polycrystal but single-phase samples, and indicate that for $\varepsilon\lesssim\varepsilon_G$ the critical exponent of $\Delta\chi(\varepsilon)$ increases somewhat,[4,43] in agreement with the predictions of the 3D XY model:[1-3,32,55]

$$\Delta\sigma_a(\varepsilon)=A_\sigma^c\varepsilon^{-1/3} \tag{19}$$

and

$$\Delta\chi_{ab}(\varepsilon)/T=A_\chi^c\varepsilon^{-2/3} \ . \tag{20}$$

Taking into account their scaling at ε_G with the mean-field expressions [Eqs. (9) and (10)], it is easy to deduce that the reduced temperature-independent amplitudes A_σ^c and A_χ^c are given by

$$A_\sigma^c=A_\sigma\left[1+\frac{B_\sigma}{\varepsilon_G}\right]^{-1/2}\varepsilon_G^{-2/3} \tag{21}$$

and

$$A_\chi^c=A_\chi\left[1+\frac{B_\chi}{\varepsilon_G}\right]^{-1/2}\varepsilon_G^{-1/3} \ . \tag{22}$$

By combining Eqs. (19)–(22), we obtain for $\varepsilon\lesssim\varepsilon_G$

$$\frac{\Delta\chi_{ab}(\varepsilon)/T}{\Delta\sigma_a(\varepsilon)}=\frac{A_\chi}{A_\sigma}\varepsilon_G^{1/3}\varepsilon^{-1/3} \ , \tag{23}$$

a relationship that, in contrast with Eq. (16) for the mean-field regime, depends on $\varepsilon^{-1/3}$. This is, in fact, the behavior qualitatively observed in Fig. 8. However, we must conclude this analysis by stressing that, as noted before, the present results for $\varepsilon\lesssim 10^{-2}$ may be strongly affected by the presence of small stoichiometric inhomogeneities in our samples. Measurements in crystals with different oxygenation treatments will help to separate the intrinsic critical effects from the spurious $\chi(T)$ and $\rho(T)$ deformations very close to the transition.

V. CONCLUSIONS

In this paper we have presented detailed experimental results on the magnetic susceptibility of high-quality $YBa_2Cu_3O_{7-\delta}$ single crystals for the applied magnetic field H parallel, χ_{ab}, and perpendicular, χ_c, to the c direction. The data were obtained from 5 to 300 K, and with $\mu_0 H\lesssim 0.6$ T, for which χ_{ab} and χ_c above the superconducting transition correspond to the so-called weak magnetic-field limit, even for reduced temperatures $\varepsilon\equiv(T-T_{CO})/T_{CO}$, of the order of $\varepsilon=2\times10^{-3}$, where T_{CO} is the mean-field-like normal-superconducting transition temperature. T_{CO} in this weak magnetic field limit is approximated as the temperature where χ_c, which is not appreciably affected by rounding effects above the transition, goes through zero, and for the four samples studied here is between 89 and 91 K. For $T>T_{CO}$, χ_c is found to be temperature independent and its average value for the samples measured here is $(2.7\pm0.5)\times10^{-5}$. In contrast, $\chi_{ab}(T)$ is found to be temperature independent, and equal to $(5.2\pm1)\times10^{-5}$, only above $T-T_{CO}\approx 25$ K and up to the highest temperature studied here (300 K). Between T_{CO} and $T-T_{CO}\approx 25$ K, $\chi_{ab}(T)$ is appreciably rounded. These values for the susceptibility in the normal region far from T_{CO} are relatively similar (to within 20%) to those obtained in other measurements in single crystals[40] and in single-phase aligned powder[16] or ceramic samples[4,41] (in this last case by taking into account the random orientation of the different sample domains), and they are also reasonably close to those calculated by other authors on the grounds of the SDFA-RPA approach.[42] The excess diamagnetism above but near T_{CO}, for H parallel to the c axis, $\Delta\chi_{ab}$, was extracted from these data following a consistent procedure and analyzed in terms of the existing approaches for independent Gaussian fluctuations of the superconducting-order-parameter amplitude in layered materials. These data were also compared with the paraconductivity extracted from measurements of the electrical resistivity in the a direction of the same samples. The main conclusions of this analysis and comparison are (i) in agreement with our previous results obtained from measurements of the magnetic susceptibility

and of the electrical resistivity in single phase polycrystalline $YBa_2Cu_3O_{7-\delta}$ samples, the so-called mean-field-like region (MFR) will correspond to, approximately, $10^{-2} \lesssim \varepsilon \lesssim 0.15$. Beyond the lower ε limit, closer to T_{CO}, the measurements may be strongly affected by the presence of small stoichiometric inhomogeneities. However, the critical exponent for $\Delta\chi_{ab}(\varepsilon)$ is compatible with the value $-\frac{2}{3}$, the exponent expected from scaling approaches for the static critical region.[55] (ii) A scenario compatible not only with the experimental results presented here on the amplitude and ε behavior of $\Delta\chi_{ab}(\varepsilon)$, and with an inappreciable $\Delta\chi_c$, but also with the paraconductivity measured in the same samples, corresponds to a complex order parameter with two real components, i.e., conventional ${}^1s_0$-wave pairing or one complex component unconventional pairing, $\xi_{ab}(0)=(1.1\pm0.2)$ nm, $\xi_c(0)=(0.12\pm0.02)$ nm, two CuO_2 superconducting layers, with the same Josephson coupling strength, in the unit-cell length, and $\varepsilon_G \approx 10^{-2}$. The fact that $B_{\sigma,\chi}$ is of the order of 0.15, indicates that in this scenario the OPF effects in $YBa_2Cu_3O_{7-\delta}$ compounds have a 2D-3D transition in the high-temperature side of the MFR, and that the OPF are 3D in nature in most of the MFR. Also, in this scenario the measured paraconductivity may be explained by direct OPF effects, i.e., the possible pair-breaking (Maki-Thompson) contributions to the electrical conductivity seem to be negligible in all the MFR. To within the corresponding experimental uncertainties, the existing results for the upper critical magnetic-field amplitudes and for the Ginzburg-Landau effective mass[56–59] are found to be fairly compatible with the above-indicated characteristic lengths and parameters. However, measurements of these last observables in the same samples for which we have measured $\Delta\sigma$ and $\Delta\chi$ are now under way to try to eliminate the remaining ambiguities and to make then such a comparison more quantitative.

ACKNOWLEDGMENTS

This work has been supported by the Comisión Interministerial de Ciencia y Tecnología (MAT88-0769 and MAT92-0841), the Programa MIDAS, and the Fundación Ramón Areces, Spain. We also thank J. Jegoudez and A. Revcolevschi for two of the single crystals measured in this work, and M. V. Ramallo and E. González for their contribution to the data analysis and to the comparison with the theory.

[1]See, e.g., W. J. Skocpol and M. Tinkham, Rep. Prog. Phys. **38**, 1049 (1975), and references therein.

[2]See, e.g., L. N. Bulaevskii, V. L. Ginzburg, and A. A. Sobyanin, Physica C **152**, 378 (1988), and references therein.

[3]D. S. Fisher, M. P. A. Fisher, and D. A. Huse, Phys. B **43**, 130 (1991).

[4]F. Vidal, C. Torrón, J. A. Veira, F. Miguélez, and J. Maza, J. Phys. Condens. Matter **3**, L5219 (1991); **3**, 9257 (1991); C. Torrón, O. Cabeza, J. A. Veira, J. Maza, and F. Vidal, *ibid.* **4**, 4273 (1992).

[5]N. P. Ong, Z. Z. Wang, S. Hagen, T. W. Jing, J. Clayhold, and J. Horvath, Physica C **153-155**, 1072 (1988); S. J. Hagen, T. W. Jing, Z. Z. Wang, J. R. Horvath, and N. P. Ong, Phys. Rev. B **37**, 7928 (1988); S. J. Hagen, Z. Z. Wang, and N. P. Ong, *ibid.* **38**, 7137 (1988).

[6]T. A. Friedmann, J. P. Rice, J. Giapintzakis, and D. M. Ginsberg, Phys. Rev. B **39**, 4258 (1989); T. A. Friedmann, M. W. Ravin, J. Giapintzakis, J. P. Rice, and D. M. Ginsberg, *ibid.* **42**, 6217 (1990); J. P. Rice, J. Giapintzakis, D. M. Ginsberg, and J. M. Mochel, *ibid.* **44**, 10 158 (1991); J. P. Rice and D. M. Ginsberg, *ibid.* **46**, 12 049 (1992).

[7]M. Hikita, Y. Tajima, H. Fuke, K. Sugiyama, M. Date, and A. Yamagishi, J. Phys. Soc. Jpn. **58**, 2248 (1989); M. Hikita and M. Suzuki, Phys. Rev. B **39**, 4756 (1989); **41**, 834 (1990).

[8]G. Weigang and K. Winzer, Z. Phys. B **77**, 11 (1989); G. Kumm and K. Winzer, Physica B **165-166**, 1361 (1990); K. Winzer and G. Kumm, Z. Phys. B **82**, 317 (1991).

[9]K. Semba, T. Ishii, and A. Matsuda, Phys. Rev. Lett. **67**, 769 (1991).

[10]N. Overend and M. A. Howson, J. Phys. Condens. Matter **4**, 9615 (1992).

[11]C. Baraduc, V. Pagnon, A. Buzdin, J. Y. Henry, and C. Ayache, Phys. Lett. A **166**, 267 (1992).

[12]C. Torrón, A. Díaz, J. Jegoudez, J. Maza, A. Pomar, A. Revcolevschi, J. A. Veira, and F. Vidal, Physica C **212**, 440 (1993); Physica B (to be published). Some partial results on the magnetic susceptibility above the superconducting transition of $YBa_2Cu_3O_{7-\delta}$ single crystals are also presented here.

[13]A. Pomar, A. Díaz, M. V. Ramallo, C. Torrón, J. A. Veira, and F. Vidal, Physica C **218**, 257 (1993).

[14]P. P. Freitas, C. C. Tsuei, and T. S. Plaskett, Phys. Rev. B **36**, 833 (1987).

[15]K. Kanoda, T. Takahashi, T. Kawagoe, T. Mizoguchi, M. Hasumi, and S. Kagoshima, Physica C **153-155**, 749 (1988); J. Phys. Soc. Jpn. **57**, 1554 (1988).

[16]W. C. Lee, R. A. Klemm, and D. C. Johnston, Phys. Rev. Lett. **63**, 1012 (1989); W. C. Lee and D. C. Johnston, Phys. Rev. B **41**, 1904 (1990).

[17]U. Welp, S. Flesher, W. K. Kwok, R. A. Klemm, V. M. Vinokur, J. Downey, B. Veal, and G. W. Crabtree, Phys. Rev. Lett. **67**, 3180 (1991).

[18]M. A. Obolenskii, A. V. Bondarenko, V. I. Beletskii, V. N. Morgun, V. N. Popov, N. N. Chebotaev, I. V. Svechkarev, A. S. Panfilov, A. A. Smirnof, O. A. Mironov, S. V. Chistyakov, and I. Yu Skrilev, Sov. J. Low Temp. Phys. **16**, 332 (1990).

[19]A. V. Volkozub, O. V. Snigirev, I. N. Makarenko, and S. M. Stishov, Pis'ma Zh. Eksp. Teor. Fiz. **54**, 274 (1991) [JETP Lett. **54**, 268 (1991)].

[20]See, e.g., S. Ullah and A. T. Dorsey, Phys. Rev. B **44**, 262 (1991).

[21]See, e.g., M. B. Salamon and J. Shi, Phys. Rev. Lett. **69**, 1622 (1992); U. Welp, S. Flesher, W. K. Kwok, R. A. Klemm, V. M. Vinokur, J. Downey, B. Veal, and G. W. Crabtree, *ibid.* **69**, 1623 (1992).

[22]See, e.g., J. A. Veira and F. Vidal, Physica C **159**, 468 (1989).

[23]R. A. Klemm, Phys. Rev. B **41**, 2073 (1990).
[24]J. F. Annett, N. Goldenfeld, and S. R. Renn (private communication).
[25]H. Schmidt, Z. Phys. **216**, 336 (1968); see also, A. Schmid, Phys. Rev. **180**, 527 (1969).
[26]W. E. Lawrence and S. Doniach, in *Proceedings of the Twelfth International Conference on Low-Temperature Physics,* Kyoto, Japan, 1970, edited by E. Kanda (Keigatu, Tokyo, 1971), p. 361.
[27]K. Maki and R. S. Thompson, Phys. Rev. B **39**, 2769 (1989).
[28]S. K. Yip, Phys. Rev. B **41**, 2612 (1990); J. Low Temp. Phys. **81**, 129 (1990).
[29]L. G. Aslamazov and H. I. Larkin, Phys. Lett. **26A**, 238 (1968).
[30]C. Baraduc and A. Buzdin, Phys. Lett. A **171**, 408 (1992).
[31]L. Reggiani, R. Vaglio, and A. A. Varlamov, Phys. Rev. B **44**, 9541 (1991); A. A. Varlamov and L. Reggiani, *ibid.* **45**, 1060 (1992).
[32]M. V. Ramallo *et al.* (unpublished).
[33]L. F. Schneemeyer, J. V. Waszczak, T. Siegrist, R. B. van Dover, L. W. Rupp, B. Batlogg, R. J. Cava, and D. W. Murphy, Nature **328**, 601 (1987).
[34]J. P. Rice, B. G. Pazol, D. M. Ginsberg, T. J. Moran, and M. B. Weissman, J. Low Temp. Phys. **72**, 345 (1988).
[35]D. Favrot, Ph.D. thesis, University of Paris-Sud, Orsay, France, 1992 (unpublished).
[36]J. P. Rice, E. D. Bukowski, and D. M. Ginsberg, J. Low Temp. Phys. **77**, 119 (1989).
[37]G. W. Crabtree, K. W. Kwok, U. Welp, A. Umezawa, K. G. Vandervoort, S. Flesher, J. Downey, Y. Fang, and J. Liu, in *Proceedings of the International Workshop on Electronic Properties and Mechanisms in High-T_c Superconductors,* Tsukuba, Japan, 1991, edited by T. Oguchi, K. Kadowaki, and T. Sasaki (North-Holland, Amsterdam, 1992), p. 193.
[38]A. A. Abrikosov and L. P. Gor'kov, Zh. Eksp. Teor. Fiz. **39**, 1781 (1961) [Sov. Phys. JETP **12**, 1243 (1961)].
[39]M. Tinkham, in *Introduction to Superconductivity* (McGraw-Hill, New York, 1975), Chap. 8.
[40]K. Fukuda, S. Shamoto, M. Sato, and K. Oka, Solid State Commun. **65**, 1323 (1988).
[41]G. Triscone, J.-Y. Genoud, T. Graf, A. Junod, and J. Mueller, J. Alloys Compounds **195**, 351 (1993).
[42]W. Götz and H. Winter, Solid State Commun. **82**, 457 (1992).
[43]J. A. Veira and F. Vidal, Phys. Rev. B **42**, 8748 (1990).
[44]J. A. Veira, C. Torrón, J. Maza, and F. Vidal, Physica B **165-166**, 1367 (1990).
[45]See, e.g., O. Cabeza, A. Pomar, A. Díaz, C. Torrón, J. A. Veira, J. Maza, and F. Vidal, Phys. Rev. B **47**, 5332 (1993); J. Phys. Condens. Matter **5**, 1365 (1993).
[46]A. G. Aronov, S. Hikami, and A. I. Larkin, Phys. Rev. Lett. **62**, 965 (1989).
[47]J. B. Bieri and K. Maki, Phys. Rev. B **42**, 4854 (1990).
[48]R. S. Thompson, Phys. Rev. Lett. **66**, 2280 (1991).
[49]J. B. Bieri, K. Maki, and R. S. Thompson, Phys. Rev. B **44**, 4709 (1991).
[50]E. Bonjour, R. Calemczuk, J. Y. Henry, and F. Khoder, Phys. Rev. B **43**, 106 (1991); A. Junod, in *Physical Properties of High Temperature Superconductors II,* edited by D. M. Ginsberg (World Scientific, Singapore, 1990), Chap. 2.
[51]See, e.g., S. E. Inderhees, M. B. Salamon, J. P. Rice, and D. M. Ginsberg, Phys. Rev. Lett. **66**, 232 (1919), and references therein.
[52]See, e.g., B. Batlogg, in *Physics of High Temperature Superconductors,* edited by S. Maekawa and M. Sato (Springer-Verlag, Berlin, 1992), p. 219.
[53]See, e.g., D. K. Finnemore, in *Phenomenology and Applications of High-Temperature Superconductors,* edited by K. S. Bedill, M. Inni, D. Meltzer, J. R. Schieffer, and S. Doniach (Addison-Wesley, New York, 1992), p. 164.
[54]See, e.g., J. Maza and F. Vidal, Phys. Rev. B **43**, 10 560 (1991), and references therein.
[55]C. J. Lobb, Phys. Rev. B **36**, 3930 (1987); M. L. Kulić and H. Stenschke, Solid State Commun. **66**, 497 (1988); A. Kapitulnik, M. R. Beasley, C. Castellani, and C. Di Castro, Phys. Rev. B **37**, 537 (1988).
[56]U. Welp, M. Grimsditch, H. You, W. K. Kwok, M. M. Fang, G. W. Crabtree, and J. Z. Liu, Physica C **161**, 1 (1989).
[57]T. T. M. Palstra, B. Batlogg, L. F. Schneemeyer, and J. W. Waszczak, Phys. Rev. Lett. **64**, 3090 (1990).
[58]D. R. Harshman, L. F. Schneemeyer, J. W. Waszczak, G. A. Aepli, R. J. Cava, B. Batlogg, L. W. Rupp, E. J. Ansaldo, and D. Ll. Williams, Phys. Rev. B **39**, 851 (1989).
[59]D. E. Farrell, J. P. Rice, D. M. Ginsberg, and J. Z. Liu, Phys. Rev. Lett. **64**, 1573 (1990).